The 2012 World Congress on
Advances in Civil, Environmental, and Materials Research (ACEM' 12)
Seoul, Korea, August 26-30, 2012

A Pragmatic Receipt for the Stability Analysis of Solution Strategies for Coupled Multi-Field Problems

*Seyedmohammad Zinatbakhsh[1)], Bernd Markert[2)] and Wolfgang Ehlers[3)]

[1), 2), 3)] *Institute of Applied Mechanics (Civil Engineering), University of Stuttgart, Pfaffenwaldring 7, 70569 Stuttgart, Germany*
[1)] *zinat@mechbau.uni-stuttgart.de*

ABSTRACT

The systems of coupled partial differential equations (PDE) are usually solved numerically, following a monolithic or decoupled solution algorithm. Despite the capability of the monolithic schemes in resulting unconditionally stable numerical solutions, these solvers are very case-specific and only semi-optimal. This has motivated the development of various decoupled solution strategies. However, decoupling of the problem can cause conditional stability of the solution and therefore, must be accompanied by an exhaustive stability analysis.

Here, we endeavour to propose a feasible receipt for the stability analysis of staggered and partitioned solution strategies applied to coupled, multi-field problems. The procedure is used to obtain the stability conditions of decoupled solution schemes applied to the problems of thermoelastodyanmics as well as fluid-porous media interaction.

1. INTRODUCTION

1) Post Graduate Student
2) Senior Lecturer (Privatdozent)
3) Professor

Dynamic interaction among distinct heterogeneous components yields a coupled phenomenon. This interaction can occur throughout the volume, as in thermo-mechanical coupling (REF) and solid-pore fluid interaction (REF), or on a surface interface, as in fluid-structure interaction (REF). Therefore, the coupled problems can be divided into volume- and surface-coupled problems (Markert2010). The mathematical modelling of these problems often results in systems of coupled partial differential equations (PDE) in space and time the solution of which reveals the response to excitations or changes in the external conditions. This is usually done numerically and following a monolithic or a decoupled solution scheme \cite{H.1995,Bathe1995, Piperno1995, degroote2008}, \cite{ Armero1992,Argyris1982} \cite{Zien1988, Maea2009}.

The monolithic solvers are based on a holistic solution of the system and employing an implicit time integration, they result in unconditionally stable numerical solutions \cite{Armero1992}. However, these schemes are very case-specific and often only semi-optimal. Moreover, they usually yield large equation systems. On the contrary, in the partitioned approaches, the physically or computationally heterogeneous system components are treated as isolated entities that are independently advanced in time, possibly by different integrators. This can be done, e.g., by accomplishing the time integration and data transfer in the sense of the block-Gauss-Seidel strategy [17, 41] or the Conventional Serial Staggered (CSS) procedure [1, 15], or using localised Lagrange multiplier method (REF). Using a decoupled solve facilitates the possibility of exploiting tailored discretisation and solution algorithms for individual subsystems and of using non-matching models for the interacting fields as well as software re-usability

and the capability of taking advantage of specialised codes \cite{Feea2001,Farhat2000}. Nevertheless, selection of the way of partitioning and the sequence of time integration of the subsystems can be detrimental to the stability of the scheme and can lead to conditional stability \cite{Matthies2006, Joosten2009}. Consequently, stability analysis and establishing the stability condition become pertinent steps in proposing new decoupled solution strategies. It has been the motivation for many case-specific applications, for example in \cite {Zien1988} and \cite{Park1983}, the stability of staggered solution algorithms applied to pore fluid-soil interaction problems is investigated. Moreover, in \cite{Armero1992}, the von Neumann stability analysis method is employed to provide the necessary stability condition for an isothermal operator-splitting scheme that has been proposed for the decoupled solution of a thermomechanical problem. In \cite{degroote2008}, the Fourier error analysis is used to achieve the stability condition of a partitioned solution scheme applied to the coupled problem of an unsteady flow in a tube, while in \cite{Joosten2009}, the block Gauss-Seidel method is employed to solve FSI in a staggered fashion and to investigate the influence of different time integrators on the convergence.

However, despite the vast number of stability-analysis-related publications, usually either a proper explanation of the procedure is missing or authors interpret the method in a rather mathematical way that makes it puzzling for researchers from more application-oriented disciplines. To this end, the present study endeavours to overcome these deficiencies and proposes a stability analysis algorithm that incorporates the salient features of the previous works. The focus is on providing a procedure that can be employed to find the critical grid sizes in different scenarios with minimum difficulty

and without any need to solve the problem. To illustrate its capabilities, the algorithm is then utilised for the stability analysis of solution schemes applied to surface- and volume-coupled multi-field problems.

The paper is organised as follows. In Section (2), the stability analysis algorithm is presented. In Section (3), the method is employed to investigate the stability conditions of decoupled solution schemes used to solve the coupled problems of 1-d and 2-d thermoelastodynamics as well as fluid-porous media interaction. Finally, the conclusion and discussion are presented in Section~\ref{sec:Concl}.

2. STABILITY ANALYSIS ALGORITHM

Assume that the mathematical modelling of a transient physical phenomenon happening on some specific d-dimensional spatial domain $\Omega \subset R^d$ and time interval $[t_0, T]$yields a hyperbolic or parabolic PDE system in space and time, which in abstract form reads

$$L\underline{U}(\underline{x},t) = \underline{F}, \qquad \forall \underline{x} \in \Omega, \qquad t_0 \le t \le T. \tag{1}$$

Therein, L represents some differential operator of space and time and $\underline{U} \in R^P$ is the unknown state vector, containing p primary variables for which (1) has to be solved. Considering the standard 3-dimensional physical space and replacing all the derivatives by differential quotients changes (1) to a system of coupled algebraic finite-difference equations (FDE) that, assuming a constant and uniform grid in space and time, for each grid point at time $t^n = n\Delta t$ and position $\underline{x}_{jkl} = [j\Delta x_1, k\Delta x_2, l\Delta x_3]$reads

$$D(\underline{X}^n_{jkl}) = \underline{F}^n_{jkl}, \tag{2}$$

where D represents some finite-difference operator approximating L, $(.)_{jkl}^{n} := (.)\big|_{\underline{x}=\underline{x}_{jkl}}^{t=t^n}$ and $\underline{\mathrm{X}}_{jkl}^{n}$ is an approximation of $\underline{U}_{jkl}^{n}$ that has to be calculated via numerical computation. Moreover, from the inverse Fourier transform, we have

$$\underline{\mathrm{X}}_{jkl}^{n} = \frac{1}{\sqrt{2\pi}} \int_{-\pi/\Delta x_1}^{\pi/\Delta x_1} \int_{-\pi/\Delta x_2}^{\pi/\Delta x_2} \int_{-\pi/\Delta x_3}^{\pi/\Delta x_3} e^{i(j+k+l)\vartheta}\, \underline{\hat{\mathrm{X}}}^{n}(\xi_1,\xi_2,\xi_3)\, d\xi_1 d\xi_2 d\xi_3 \qquad (3)$$

with $i := \sqrt{-1}$, $\vartheta \in [-\pi, \pi]$ and $\xi_a := \vartheta / \Delta x_a$ for $a = \{1,2,3\}$. Then, following the method proposed in (REF) one obtains

$$\underline{\hat{\mathrm{X}}}^{n+1} = \underline{G}(\Delta t, \Delta \underline{x})\underline{\hat{\mathrm{X}}}^{n} \rightarrow \underline{\hat{\mathrm{X}}}^{n} = \left[\underline{G}(\Delta t, \Delta \underline{x})\right]^{n} \underline{\hat{\mathrm{X}}}^{0} \qquad (4)$$

where $0 \le n \le T/\Delta t$ and $\underline{G}$ is called the amplification matrix. Consequently, the necessary and sufficient stability condition for the numerical scheme reads (REF)

$$\exists C_1 \in R \;\big|\; \left\|\underline{G}^{n}\right\| \le C_1 \qquad (5)$$

with $\left\|\underline{G}\right\| := \underset{|\underline{v}|=1}{SUP} |\underline{G}\underline{v}|$. Moreover, the spectral radius P is defined as the biggest eigenvalue of the amplification matrix in the absolute form. Then, it can be shown that (REF)

$$\mathrm{P}^{n} \le \left\|\underline{G}^{n}\right\|. \qquad (6)$$

Hence, a necessary stability condition for the numerical solution scheme reads

$$\exists C_2 \in R \;\big|\; \mathrm{P}^{n} \le C_2. \qquad (7)$$

Assuming $C_2 \ge 1$, one concludes

$$\mathrm{P} \le C_2^{1/n} \xrightarrow{\forall n \in [0, T/\Delta t]} \mathrm{P} \le C_2^{\Delta t/T} \approx 1 + \mathrm{O}(\Delta t), \qquad (8)$$

which is known as the von Neumann stability criterion (REF). Accordingly, $\mathrm{P} < 1$ is a sufficient condition to satisfy (8) and to guarantee the boundness of the spectral radius. Hence, the conditions under which all roots of the characteristic equation, associated

with the amplification matrix, lie on the unit circle on the complex plane, is known as the necessary stability condition for the solution scheme (REF). This condition may directly be checked by assembling the characteristic equation, known as the amplification polynomial, and computing its roots. However, it is mostly desired to determine the necessary stability condition solely based on the coefficients of the amplification polynomial, thus, avoiding the explicit computation of the roots. The Schur-Cohn stability criterion is a plausible way to directly compute this condition. Having the amplification polynomial as an algebraic polynomial of order $n \geq 1$, the Schur-Cohn matrix $\underline{D}$ reads

$$\underline{D} = \begin{bmatrix}
\alpha_n & \alpha_{n-1} & \cdots & \alpha_2 & \alpha_1 & 0 & 0 & \cdots & 0 & \alpha_0 \\
0 & \ddots & & & \vdots & & & & \iddots & \vdots \\
\vdots & & \alpha_n & \alpha_{n-1} & \alpha_{n-2} & 0 & 0 & \alpha_0 & & . \\
. & & 0 & \alpha_n & \alpha_{n-1} & 0 & \alpha_0 & \alpha_1 & & . \\
. & & 0 & 0 & \alpha_n & \alpha_0 & \alpha_1 & \alpha_2 & & . \\
. & & 0 & 0 & \overline{\alpha}_0 & \overline{\alpha}_n & \overline{\alpha}_{n-1} & \overline{\alpha}_{n-2} & & . \\
. & & 0 & \overline{\alpha}_0 & \overline{\alpha}_1 & 0 & \overline{\alpha}_n & \overline{\alpha}_{n-1} & & . \\
\vdots & & \overline{\alpha}_0 & \overline{\alpha}_1 & \overline{\alpha}_2 & 0 & 0 & \overline{\alpha}_n & & . \\
0 & \iddots & & & \vdots & & & & \ddots & \vdots \\
\overline{\alpha}_0 & \overline{\alpha}_1 & \cdots & \overline{\alpha}_{n-2} & \overline{\alpha}_{n-1} & 0 & 0 & \cdots & 0 & \overline{\alpha}_n
\end{bmatrix} \tag{9}$$

where α_i represents the coefficients of the amplification polynomial

$$G_A(\gamma) := \det(\underline{G} - \gamma \underline{I}) = \alpha_0 + \alpha_1 \gamma + \cdots + \alpha_{n-1} \gamma^{n-1} + \alpha_n \gamma^n \tag{10}$$

and $\overline{\alpha}_i$ is the complex conjugate of α_i. Following that, the Schur-Cohn criterion (SCC) reads: "*all the roots of the amplification polynomial lie on or inside the unit circle on the complex plane if and only if the Schur-Cohn matrix is positive innerwise*." (REF33,34).

However, to directly check the SCC can be computationally very expensive (REF Felippa and Park). Instead, one transforms the amplification polynomial to a Hurwitz polynomial to alleviate this problem (REF16). This is done by changing the variable from γ to s using the following map:

$$\gamma = \frac{1+s}{1-s} \quad \rightarrow \quad G_A(\gamma) = G_A\left(\frac{1+s}{1-s}\right) =: \frac{G_H(s)}{D_H(s)}. \tag{11}$$

Doing so and suppressing all common factors, satisfaction of the von Neumann stability criterion becomes equivalent to having negative real parts for all the roots of the Hurwitz polynomial $G_H(s)$. This condition can be checked via the Routh-Hurwitz criterion (RHC) (REF 35, 36), which reads: "*All the roots of the Hurwitz polynomial lie on the left half-plane if and only if all of the Hurwitz determinants corresponding to* $G_H(s)$ *are positive*".

It should be noted that for $G_H(s) = \sum_{i=0}^{n} \beta_i s^i$ the Hurwitz determinant is defined as

$$\Delta_i := \begin{vmatrix} \beta_1 & \beta_3 & \beta_5 & \cdots & \beta_{2i-1} \\ \beta_0 & \beta_2 & \beta_4 & \cdots & \beta_{2i-2} \\ 0 & \beta_1 & \beta_3 & \cdots & \beta_{2i-3} \\ 0 & \beta_0 & \beta_2 & \cdots & \beta_{2i-4} \\ . & . & . & \cdots & \\ . & . & . & \cdots & \beta_i \end{vmatrix}. \tag{12}$$

Although the RHC is easier to handle than the SCC, the evaluation of all Hurwitz determinants still proves difficult. A more practical criterion that essentially yields the same result (REF38) is the one proposed by Liénard and Chipart in 1914 (REF38). The so-called Liénard-Chipart criterion (LCC) assures that the necessary stability condition

is satisfied if and only if the corresponding expressions represented in Table (REF) are all positive.

Table 1: Expressions for the Liénard-Chipart stability criterion.

Order	Expression
1	$\beta_0,\ \beta_1$
2	$\beta_0,\ \beta_1,\ \beta_2$
3	$\beta_0,\ \beta_1,\ \Delta_2,\ \beta_3$
4	$\beta_0,\ \beta_1,\ \Delta_3,\ \beta_3,\ \beta_4$
5	$\beta_0,\ \beta_1,\ \Delta_2,\ \beta_3,\ \Delta_4,\ \beta_5$
6	$\beta_0,\ \beta_1,\ \Delta_3,\ \beta_3,\ \Delta_5,\ \beta_5,\ \beta_6$

In conclusion, the flowchart provided in Figure 1 can be used to obtain the necessary stability condition for general numerical solution schemes applied to coupled PDE systems.

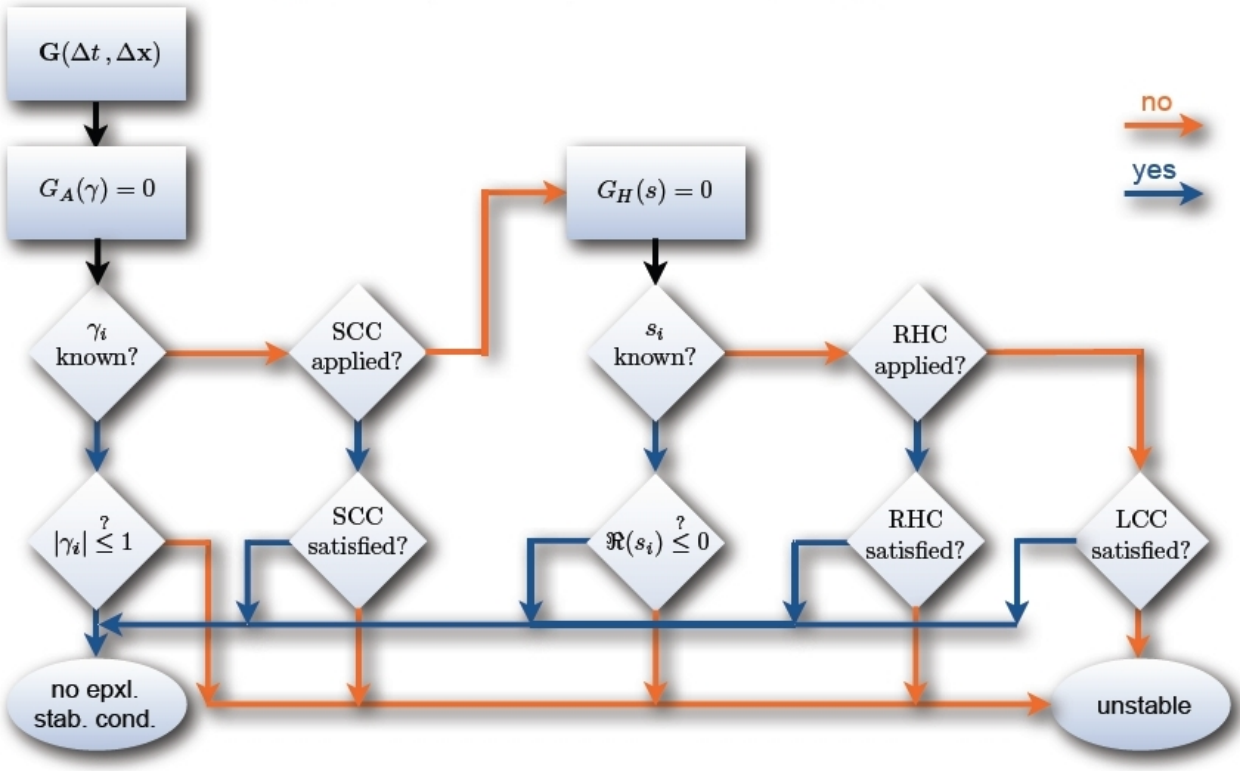

Figure 1: Stability analysis flowchart.

3. Applications

In this section, the stability analysis algorithm introduced before is used to investigate the stability condition of decoupled solution schemes applied on coupled problem of Thermoelastodynamics and fluid-porous media interaction.

3.1. Linear Thermoelastodynamics

In this section, the volume-coupled problem of thermoelastodynamicsis is studied. The proposed decoupled solution scheme is based on the block Gauss-Seidel strategy for data transfer between subsystems (Armero). The necessary stability conditions for

1- and 2-d problems are established.

3.1.1 System of governing equations The linear momentum balance, together with the energy balance compose the governing equation system for the problem of thermoelastodynamics. For the geometrically linear regime and neglecting body forces and radiation terms it reads (REF7)

$$X:\begin{cases}\dot{\underline{u}} = \underline{v}, \\ \dot{\underline{v}} = \dfrac{1}{\rho} div(\underline{\sigma}), \\ \dot{\theta} = -\dfrac{1}{\rho C_v}\left[m\theta_0 div(\underline{v}) + div(\underline{q})\right], \end{cases} \tag{13}$$

where the first equation is just added to obtain a 1st-order equation system in time. This facilitates the application of established numerical integration schemes out of the class of Runge-Kutta methods. Furthermore, a superposed dot represents the total derivative w.r.t. time, ρ is the mass density, C_v is the specific heat at constant volume, m is the stress-temperature modulus and θ_0 is the reference temperature. The constitutive relations for the stress tensor and heat transfer vector read

$$\begin{cases}\underline{\sigma} = 2\mu\underline{\varepsilon} + \lambda(\underline{\varepsilon}\cdot\underline{I})\underline{I} - m\Delta\theta\underline{I}, \\ \underline{q} = -k\left[grad(\theta)\right], \end{cases} \tag{14}$$

where μ and λ are the Lamé constants and k the thermal conductivity. Furthermore, $\underline{\varepsilon}$ represents the strain tensor in the linear regime

$$\underline{\varepsilon} := \frac{1}{2}\left[grad(\underline{u}) + grad^T(\underline{u})\right] \tag{15}$$

3.1.2 Decoupled solution scheme Equation (13) represents a coupled PDE system, where the strength of coupling between the mechanical unknowns, i.e., displacement and velocity, and the thermal variable, i.e., temperature, is governed by the stress-temperature modulus. This equation system can easily be solved in a decoupled fashion. Here we focus on the isothermal operator-splitting method (REF 7) and employ our stability analysis algorithm to scrutinise the stability condition of this solution scheme.

The isothermal operator-splitting method is based on the block-Gauss-Seidel strategy (REF 17) and results in breaking down the problem into a mechanical subproblem, composed of Eq. $(13)_1$ and $(13)_2$, and a thermal subproblem, i.e., Eq. $(13)_3$. Then the solution is computed following a sequential procedure:

1. Insert the old value of temperature at time $t = t^n$ into the mechanical subproblem
2. Advance the mechanical subproblem and update deformation and velocity
3. Insert the newly found mechanical quantities into the thermal subproblem
4. Advance the thermal subsystem and update the temperature

Following this procedure and employing the above-described stability analysis algorithm, it can be seen that for a d-dimensional problem, the LCC is satisfied if

$$\sqrt{\sum_{i=1}^{d}\left(\frac{\Delta t}{\Delta x_i}\right)^2} \leq \frac{2\sqrt{\rho C_v / \theta_0}}{|m|}, \tag{16}$$

and hence, this is the necessary stability condition for the isothermal splitting scheme.

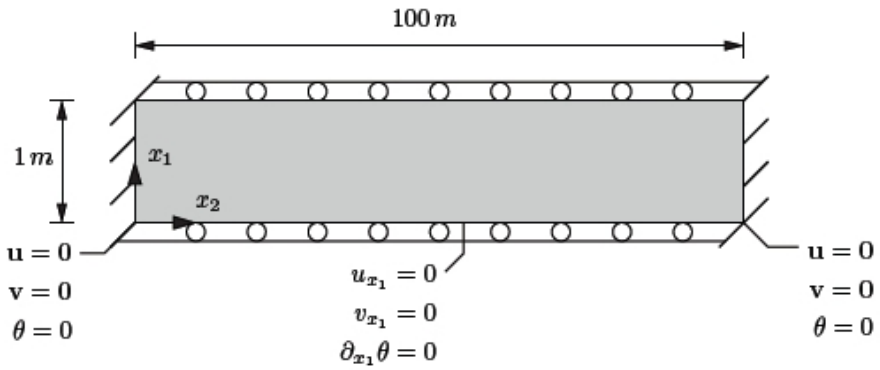

Figure 2: Geometry and boundary conditions for thermoelastic vibration (REF 7).

3.1.3 Numerical Example A thermoelastic vibration problem adopted from (REF 7) is selected to verify the results of the stability analysis. Consider a homogeneous bar with geometry and material parameters as presented in Fig. (2) and Table (2), where both ends of the bar are thermally and mechanically fixed. A perturbation in form of a sinusoidal initial velocity along the length moves the system away from its stable equilibrium state and causes a horizontal vibration, i.e.,

$$\text{Initial Conditions:} \quad \underline{u}(\underline{x},0) = \underline{0}, \quad \begin{matrix} v_{x_2}(\underline{x},0) = \sin\left(\pi x_2 / 100\right) \\ v_{x_1}(\underline{x},0) = 0 \end{matrix}, \quad \theta(\underline{x},0) = \underline{0}. \tag{17}$$

Consequently, using the material parameters as shown in Table (2) and from Eq. (16), the, critical time-step size, i.e., the biggest Δt, which satisfies the necessary

stability condition for the isothermal operator-splitting scheme reads

Table 2: Material parameters for the thermoelastic vibration problem.

Parameter	Symbol	Value	SI unit
Mass Density	ρ	1	kg/m^3
1st Lamé constant	μ	3/8	N/m^2
2nd Lamé constant	λ	6/8	N/m^2
Stress-temperature modulus	m	-1	$N/(Km^2)$
Specific heat at constant volume	C_v	1	$J/(Km^3)$

$$\Delta t_{crit.}^{1d} = 2s, \qquad \Delta t_{crit.}^{2d} = 1.15s. \tag{18}$$

In the other words, the stability analysis predicts that all roots of the amplification polynomial lie inside the unit circle on the complex plane, and the absolute value of the roots and, consequently, the spectral radius associated with the amplification matrix are less than unity as long as time-step size is smaller than the critical values in Eq. (18). It should be noted that this result has been obtained without any need to solve the problem itself. Assembling the amplification polynomial and calculating its roots verifies the correctness of this founding, see Fig. (3).

3.2. Fluid-porous media interaction

In this section, the surface-coupled problem of Fluid-Porous Media Interaction

(FPMI) is studied, see Fig. (4). The proposed decoupled solution scheme is based on the method of localised Lagrange multipliers (LLM) method, which is extensively explained and

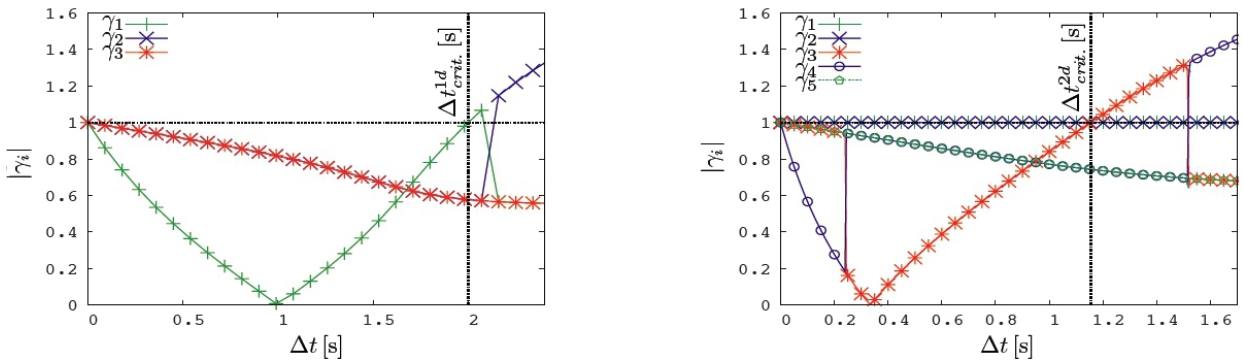

Figure 3: Roots of the amplification polynomial for 1-d (left) and 2-d (right) thermoelastic vibration problem.

implemented in (REF Park1998) and (REF Park1998b, Park2001, Park2008), to name but a few. In short, LLM method is based on breaking down the system into three

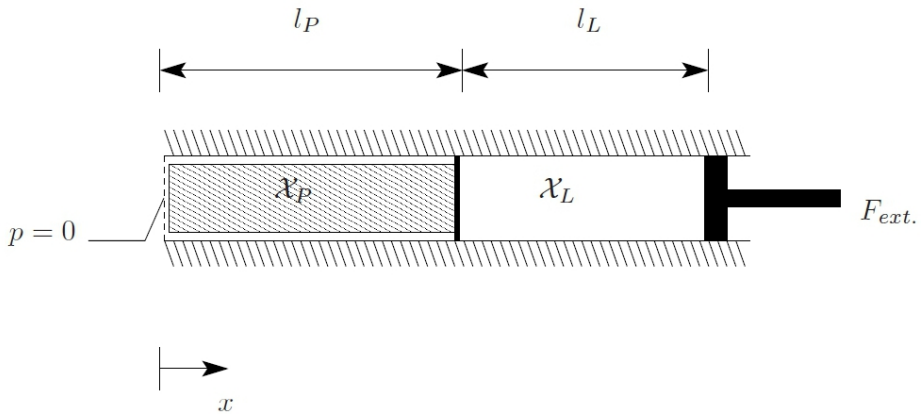

Figure 4: Schematic for the Fluid-Porous Media Interaction (FPMI)

communicating subsystems, namely, the fluid subsystem X_L , the porous media subsystem X_P and the interface. It offers a modular treatment that makes LLM method a superior candidate compared to the classical Lagrange multiplier method (REF Markert, Habil, 96, 99,100).

3.2.1 System of governing equations Here, we proceed from the interaction between an incompressible fluid with a saturated porous media, composed of intrinsically incompressible constituents. Furthermore, we assume that the membrane between the subsystems is impermeable and hence, no mass-exchange happens. Consequently, and neglecting the thermal effects and body forces, the governing equation systems for the interacting subsystems in the 1-d space and for geometrically linear regime read

$$\mathrm{X}_L : \begin{cases} \rho^L (\dot{u}_L)_{,x} = 0, \\ \rho^L \ddot{u}_L + (p_L)_{,x} = 0, \end{cases} \tag{19}$$

and

$$\mathrm{X}_P : \begin{cases} n^S (\dot{u}_S)_{,x} + n^F (\dot{u}_F)_{,x} = 0, \\ \rho^S \ddot{u}_S - E^S (\dot{u}_S)_{,xx} - \alpha(\dot{u}_F - \dot{u}_S) + n^S (p_F)_{,x} = 0, \\ \rho^F \ddot{u}_F + \alpha(\dot{u}_F - \dot{u}_S) + n^F (p_F)_{,x} = 0, \end{cases} \tag{20}$$

with

$$\alpha := \frac{(n^F)^2 \gamma^{FR}}{k^F} \tag{21}$$

and where $\rho^L = const.$ is the density of the fluid, u^L represents the displacement of the

fluid and p_L is the hydraulic pressure inside the fluid subsystem. Moreover, $\rho^a = n^a \rho^{aR}$ is the partial density of the constituent φ^a ($a = S$: solid skeleton; $a = F$: pore fluid) where $n^a := dv^a / dv$ is the volume fraction and $\rho^{aR} = const.$ is the effective or intrinsic density of φ^a. Furthermore, E^S is the Young's modulus of the porous solid matrix, γ^{FR} is the effective fluid weight and k^F represents the Darcy permeability. Moreover, $(\dot{\bullet}) := d(\bullet)/dt$, $(\ddot{\bullet}) := d^2(\bullet)/dt^2$, $(\bullet)_{,x} := \partial(\bullet)/\partial x$ and $(\bullet)_{,xx} := \partial^2(\bullet)/\partial x^2$.

3.2.2 Perturbed Lagrange multiplier formulation Both Eq. (19) and (20) are of type of Algebraic-Differential Equation (ADE) systems. Utilising perturbed Lagrange multiplier formulation (also known as the penalty function formulation) is a plausible way to eliminate the algebraic constraints and reduce the total number of equations (REF Heinrich 1995 and Park1984). To this end, one assumes that the corresponding mass balances are only weakly satisfied. Consequently the modified mass balance for X_L reads

$$\rho^L (\dot{u}_L)_{,x} = -\frac{1}{\Gamma_L} p_L \tag{22}$$

where Γ_L is called the penalty parameter and is a very large number (REF Heinrich1995). This yields a pseudo-constitutive relation for the hydraulic pressure

$$p_L = -\Gamma_L \rho^L (\dot{u}_L)_{,x} \quad \rightarrow \quad (p_L)_{,x} = -\Gamma_L \rho^L (\dot{u}_L)_{,xx}. \tag{23}$$

Replacing this result in the momentum balance of X_L yields

$$\mathrm{X}_L : \rho^L \ddot{u}_L - \Gamma_L \rho^L (\dot{u}_L)_{,xx} = 0\,, \tag{24}$$

which in the abstract form reads

$$\mathrm{X}_L : F_L(u_L) = 0. \tag{25}$$

In a similar fashion, one assumes that the representative of the mass balance for X_P, i.e., the mixture volume balance is also only weakly satisfied

$$n^S (\dot{u}_S)_{,x} + n^F (\dot{u}_F)_{,x} = -\frac{1}{\Gamma_P} p_F. \tag{26}$$

Consequently

$$p_F = -\Gamma_P \left[n^S (\dot{u}_S)_{,x} + n^F (\dot{u}_F)_{,x} \right] \quad \rightarrow \quad (p_F)_{,x} = -\Gamma_P \left[n^S (\dot{u}_S)_{,xx} + n^F (\dot{u}_F)_{,xx} \right] \tag{27}$$

Inserting this relation in the momentum balances of pore fluid and solid skeleton yields

$$\mathrm{X}_P : \begin{cases} \rho^S \ddot{u}_S - E^S (\dot{u}_S)_{,xx} - \alpha(\dot{u}_F - \dot{u}_S) - n^S \Gamma_P \left[n^S (\dot{u}_S)_{,xx} + n^F (\dot{u}_F)_{,xx} \right] = 0, \\ \rho^F \ddot{u}_F + \alpha(\dot{u}_F - \dot{u}_S) + n^F \Gamma_P \left[n^S (\dot{u}_S)_{,xx} + n^F (\dot{u}_F)_{,xx} \right] = 0. \end{cases} \tag{28}$$

that can be written in the following abstract form

$$\mathrm{X}_P : \underline{F}_P(\underline{u}_P) = \underline{0} \tag{29}$$

with $\underline{u}_p := \left[u_S, u_F \right]^T$.

3.2.3 Constraints on the interface Apart from the governing equations, one also has to make sure that additional algebraic compatibility conditions, known as the interface kinematic constraints are also satisfied. Considering Fig. (5), these compatibility conditions read

$$\begin{cases} c_1 := u_L - u_g = 0, \\ c_2 := u_S - u_g = 0, \\ c_3 := u_F - u_g = 0, \end{cases} \quad \rightarrow \quad \underline{c} := \begin{bmatrix} u_L \\ u_S \\ u_F \end{bmatrix} - \begin{bmatrix} u_g \\ u_g \\ u_g \end{bmatrix} = \underline{0} \quad \rightarrow \quad \underline{c} := \underline{\underline{B}}^T \underline{u} - \underline{\underline{L}} \underline{u}_g = \underline{0}. \tag{30}$$

Therein, $\underline{u}$ is a vector including all displacements, $\underline{u}_g$ is the global frame displacement vector, $\underline{\underline{B}}^T$ is a Boolean matrix that extracts the boundary values of the displacement and $\underline{\underline{L}}$ is the finite element assembly operator.

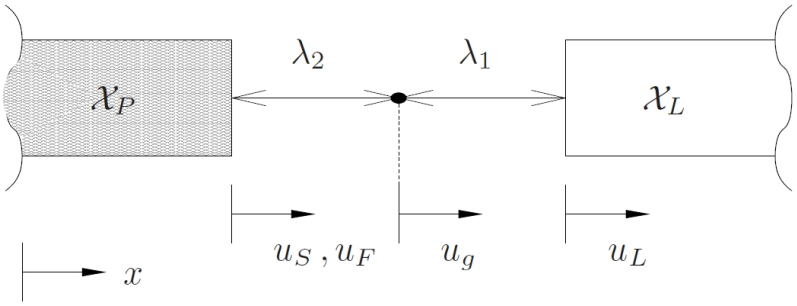

Figure 5: LLM method to decouple FPMI problem.

3.2.3 The energy functional and coupled equation system Assembling the energy functional is a key step in using the LLM method. For our problem, the energy

functional augmented with the boundary constraint condition reads

$$\Pi := \int_{V_L} F_L(u_L) u_L dV + \int_{V_P} \underline{F}_P(\underline{u}_P) \cdot \underline{u}_P^T dV + \int_S \underline{\lambda}^T \cdot \left(\underline{B}^T \underline{u} - \underline{L} \underline{u}_g \right) dA \tag{31}$$

with $\underline{\lambda} := \left[\lambda_1, \underline{\lambda}_2 \right]^T$ and $\underline{\lambda}_2 := \left[\lambda_2^S, \lambda_2^F \right]^T$ .Following that, the stationary condition $\delta\Pi(\underline{\lambda}, \underline{u}_g, u_L, \underline{u}_P) = 0$ leads the following partitioned equation system

$$\begin{cases} \dfrac{\partial \Pi}{\partial \underline{\lambda}} = \underline{B}^T \underline{u} - \underline{L} \underline{u}_g = \underline{0}, \\ \dfrac{\partial \Pi}{\partial \underline{u}_g} = -\underline{L} \cdot \underline{\lambda} = 0, \\ \dfrac{\partial \Pi}{\partial u_L} = F_L + \lambda_1 = 0, \\ \dfrac{\partial \Pi}{\partial \underline{u}_P} = \underline{F}_P + \underline{\lambda}_2 = \underline{0}. \end{cases} \tag{32}$$

It represents the decoupled equation system in the strong form. However, employing the FEM for spatial discretisation is a common practice to achieve a semi-discretised version of this equation system.

3.2.4 Governing weak formulation Following the idea of the FEM, Eq. (32) is transferred to weak formulation. To this end, the balance relations i.e., Eq. $(32)_3$ and $(32)_4$ are weighted by independent test functions and integrated over the corresponding spatial domains V_L and V_P. Moreover, the surfaces S_L and S_P are split into Dirichlet and Nuemann boundaries. Furthermore, each spatial domain is subdivided into finite number of elements yielding an approximation of the continuous domains V_L and V_P by the discrete domains V_L^h and V_P^h. This spatial discretisation

yields a finite element mesh on which the following trial functions are defined

$$u_L \approx u_L^h = \underline{U}_L \underline{u}_L, \qquad u_S \approx u_S^h = \underline{U}_S \underline{u}_S, \qquad u_F \approx u_F^h = \underline{U}_F \underline{u}_F \tag{33}$$

where $\underline{U}_L$, $\underline{U}_S$ and $\underline{U}_F$ represent the interpolation functions corresponding to the nodal unknowns of the FE mesh $\underline{u}_L$, $\underline{u}_S$ and $\underline{u}_F$. Then, multiplying each balance relation by the corresponding test function and applying the product rule and the Gaussian integral theorem, one obtains the weak forms as

$$\begin{bmatrix} \underline{M}_L \dfrac{d^2}{dt^2} - \underline{D}_L \dfrac{d}{dt} & \underline{0} & \underline{0} & \underline{B}_1 \\ \underline{0} & \underline{M}_P \dfrac{d^2}{dt^2} + \underline{D}_P \dfrac{d}{dt} + \underline{K}_P & \underline{0} & \underline{B}_2 \\ \underline{0} & \underline{0} & \underline{0} & \underline{L}^T \\ \underline{B}_1^T & \underline{B}_2^T & -\underline{L} & \underline{0} \end{bmatrix} \begin{bmatrix} \underline{u}_L \\ \underline{u}_P \\ \underline{u}_g \\ \underline{\lambda} \end{bmatrix} - \begin{bmatrix} \underline{f}_L \\ \underline{f}_P \\ \underline{0} \\ \underline{0} \end{bmatrix} = \underline{0}. \tag{34}$$

with $\underline{B} =: \begin{bmatrix} \underline{B}_1 & \underline{B}_2 \end{bmatrix}^T$. Moreover, introducing $(\bullet)^b$ to be the approximated (known) Dirichlet boundary conditions of $(\bullet)$, the mass, damping and stiffness matrices and force vectors read

$$\underline{M}_L = \rho^L \int_{V_L} \underline{U}_L^T \underline{U}_L \, dv, \qquad \underline{D}_L = \Gamma_L \rho^L \int_{V_L} (\underline{U}_L^T)_{,x} (\underline{U}_L)_{,x} \, dv, \qquad \underline{f}_L = \Gamma_L \rho^L \int_{S_L} \underline{U}_L^T (\dot{u}_L^b)_{,x} \, da. \tag{35}$$

Furthermore

$$\underline{M}_P := \begin{bmatrix} \underline{M}_S & \underline{0} \\ \underline{0} & \underline{M}_F \end{bmatrix}, \qquad \underline{D}_P := \begin{bmatrix} \underline{D}_S^1 & -\underline{D}_F^1 \\ -\underline{D}_S^2 & \underline{D}_F^2 \end{bmatrix}, \qquad \underline{K}_P := \begin{bmatrix} \underline{K}_S & \underline{0} \\ \underline{0} & \underline{0} \end{bmatrix}, \qquad \underline{f}_P := \begin{bmatrix} \underline{f}_S \\ \underline{f}_F \end{bmatrix} \tag{36}$$

with

$$
\begin{aligned}
&\underline{M}_S = \rho^S \int_{V_P} \underline{U}_S^T \underline{U}_S dv, \\
&\underline{D}_F^1 = \alpha \int_{V_P} \underline{U}_S^T \underline{U}_F dv - n^S n^F \Gamma_P \int_{V_P} (\underline{U}_S^T)_{,x} (\underline{U}_F)_{,x} dv, \\
&\underline{D}_S^1 = \alpha \int_{V_P} \underline{U}_S^T \underline{U}_S dv + (n^S)^2 \Gamma_P \int_{V_P} (\underline{U}_S^T)_{,x} (\underline{U}_S)_{,x} dv, \\
&\underline{K}_S = E^S \int_{V_P} (\underline{U}_S^T)_{,x} (\underline{U}_S)_{,x} dv, \\
&\underline{f}_S = \underline{f}_S^1 + \underline{f}_S^2 + \underline{f}_S^3, \\
&\underline{f}_S^1 = E^S \int_{S_P} \underline{U}_S^T u_{,x}^b da, \qquad \underline{f}_S^2 = (n^S)^2 \Gamma_P \int_{S_P} \underline{U}_S^T (\dot{u}_S^b)_{,x} da, \qquad \underline{f}_S^3 = n^S n^F \Gamma_P \int_{S_P} \underline{U}_S^T (\dot{u}_F^b)_{,x} da
\end{aligned}
\tag{37}
$$

and

$$
\begin{aligned}
&\underline{M}_F = \rho^F \int_{V_P} \underline{U}_F^T \underline{U}_F dv, \\
&\underline{D}_F^2 = \alpha \int_{V_P} \underline{U}_F^T \underline{U}_F dv + (n^F)^2 \Gamma_P \int_{V_P} (\underline{U}_F^T)_{,x} (\underline{U}_F)_{,x} dv, \\
&\underline{D}_S^2 = \alpha \int_{V_P} \underline{U}_F^T \underline{U}_S dv - n^F n^S \Gamma_P \int_{V_P} (\underline{U}_F^T)_{,x} (\underline{U}_S)_{,x} dv, \\
&\underline{f}_F = \underline{f}_F^1 + \underline{f}_F^2, \\
&\underline{f}_F^1 = n^S n^F \Gamma_P \int_{S_P} \underline{U}_F^T (\dot{u}_S^b)_{,x} da, \qquad \underline{f}_F^2 = (n^F)^2 \Gamma_P \int_{S_P} \underline{U}_F^T (\dot{u}_F^b)_{,x} da.
\end{aligned}
\tag{38}
$$

In the matrix form, Eq. (34) reads

$$
\underline{S} \begin{bmatrix} \underline{u} \\ \underline{u}_g \\ \underline{\lambda} \end{bmatrix} = \begin{bmatrix} \underline{f} \\ \underline{0} \\ \underline{0} \end{bmatrix}. \tag{39}
$$

3.2.5 Time discretisation Implicit time integration by the mid-point rule is an appropriate strategy for the temporal discretisation of Eq. (39). Proceeding from a time

step Δt this method reads

$$\begin{aligned} \dot{\chi}^{n+\frac{1}{2}} &= \dot{\chi}^{n} + \delta\ddot{\chi}^{1+\frac{1}{2}}, \quad \delta := \frac{\Delta t}{2}, \\ \chi^{n+\frac{1}{2}} &= \chi^{n} + \delta\dot{\chi}^{1+\frac{1}{2}}, \quad \chi^{n+1} = 2\chi^{n+\frac{1}{2}} - \chi^{n}. \end{aligned} \tag{40}$$

Then, the time discretisation of Eq. (39) leads to the following matrix discrete equation

$$\underline{S}_d \begin{bmatrix} \underline{u} \\ \underline{u}_g \\ \underline{\lambda} \end{bmatrix}^{n+\frac{1}{2}} = \begin{bmatrix} \overline{\underline{f}} \\ \underline{0} \\ \underline{0} \end{bmatrix}. \tag{41}$$

where $\overline{\underline{f}} := \begin{bmatrix} \overline{\underline{f}}_1 & \overline{\underline{f}}_2 \end{bmatrix}^T$ and

$$\underline{S}_d = \begin{bmatrix} \overline{\underline{D}}_L & \underline{0} & \underline{0} & \delta^2 \underline{B}_1 \\ \underline{0} & \overline{\underline{K}}_P & \underline{0} & \delta^2 \underline{B}_2 \\ \underline{0} & \underline{0} & \underline{0} & \underline{L}^T \\ \underline{B}_1^T & \underline{B}_2^T & -\underline{L} & \underline{0} \end{bmatrix}, \quad \begin{cases} \overline{\underline{f}}_1 := \overline{\underline{D}}_L \underline{u}_L^n + \delta \underline{M}_L \dot{\underline{u}}_L^n + \delta^2 \underline{f}_L^{n+\frac{1}{2}}, \\ \overline{\underline{f}}_2 := \overline{\underline{D}}_P \underline{u}_P^n + \delta \underline{M}_P \dot{\underline{u}}_P^n + \delta^2 \underline{f}_P^{n+\frac{1}{2}}. \end{cases} \tag{42}$$

Moreover,

$$\overline{\underline{D}}_L := \underline{M}_L - \delta \underline{D}_L, \quad \overline{\underline{D}}_P := \underline{M}_P + \delta \underline{D}_P, \quad \overline{\underline{K}}_P := \overline{\underline{D}}_P + \delta^2 \underline{K}_P. \tag{43}$$

3.2.5 An unconditionally-stable decoupled solution scheme Solving for subsystems displacements and substituting them into the interface compatibility condition one obtains

$$\begin{bmatrix} \underline{F}_b & -\underline{L} \\ \underline{L}^T & \underline{0} \end{bmatrix} \begin{bmatrix} \underline{\lambda} \\ \underline{u}_g \end{bmatrix}^{n+\frac{1}{2}} = \begin{bmatrix} \underline{g}_\lambda \\ \underline{0} \end{bmatrix}, \tag{44}$$

with

$$\begin{cases} \underline{F}_b := -\delta^2 \left(\underline{B}_1^T \overline{\underline{D}}_L^{-1} \underline{B}_1 + \underline{B}_2^T \overline{\underline{K}}_P^{-1} \underline{B}_2 \right), \\ \underline{g}_\lambda := -\left(\underline{B}_1^T \overline{\underline{D}}_L^{-1} \overline{\underline{f}}_1 + \underline{B}_2^T \overline{\underline{K}}_P^{-1} \overline{\underline{f}}_2 \right) \end{cases} \tag{45}$$

Apparently, solution of Eq.(44) reveals the new values for the interface forces and also the frame displacement. Having the updated interface forces, one can substitute them in the 1st row of Eq.(41) and consequently update the displacements of the interacting subsystems.

Employing the stability analysis algorithm discussed before, it can be shown that the LLC is always satisfied. This shows the unconditional stability of the proposed decoupled solution scheme.

3.2.6 Numerical example To set up an example, the numerical values as presented in Table (3) are chosen. It is worth mentioning that in the geometrically linear regime $n^a \approx n_{0S}^a = const.$ Using these material parameters one obtains that in spite of considering different time-step sizes, the spectral radii remains always smaller than one, see Fig. (4). It approves the unconditional stability of the solution scheme, which has previously been predicted by the stability analysis.

Table 3: Material parameters for the FPMI problem.

Parameter	Symbol	Value	SI unit
Young's modulus of the solid skeleton	E^S	$20 \cdot 10^6$	N/m^2
Volume fraction of solid	n_{0S}^S	0.67	-
Volume fraction of pore fluid	n_{0S}^F	0.33	-
Partial density of dense solid	ρ^{SR}	2000	kg/m^3
Partial density of pore fluid	ρ^{FR}, ρ^L	1000	kg/m^3
Effective fluid weight	γ^{FR}	9800	$kg/(s^2 m^2)$
Darcy permeability	k^F	10^{-2}	m/s

CONCLUSION

Enhanced and efficient 3-dimensional finite elements for the structural analysis of cable-stayed bridges …

REFERENCES

Cadappa, D.C., Sanjayan, J.G. and Setunge, S. (2001), "Complete triaxial stress-strain curves of high-strength concrete," *J. Mat. Civil Eng., ASCE,* **13**(3), 209-215.

Chern, J.C., Yang, H.J. and Chen, H.W. (1992), "Behavior of steel fiber reinforced concrete in multi axial loading", *ACI Mat. J.,* **89**(1), 32-40.

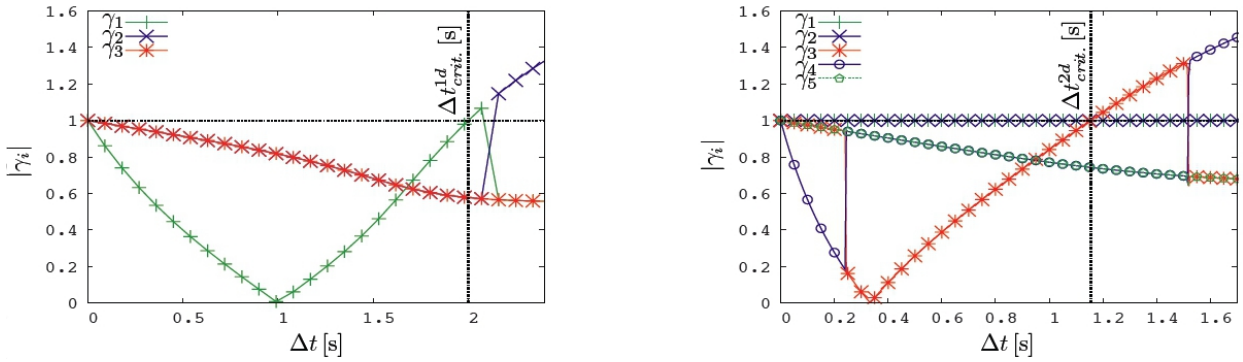

Figure 4: Spectral radii for the decoupled solution scheme proposed for FPMI problem thermoelastic vibration problem.